HHS Public Access

Author manuscript

J Eng (Stevenage). Author manuscript; available in PMC 2016 January 19.

Published in final edited form as:

J Eng (Stevenage). 2015 May ; 2015: .

Processes for design, construction and utilisation of arrays of light-emitting diodes and light-emitting diode-coupled optical fibres for multi-site brain light delivery

Jacob G. Bernstein[1,2], **Brian D. Allen**[1,2], **Alexander A. Guerra**[1,2], and **Edward S. Boyden**[+,1,2]

[1]The MIT Media Laboratory, Synthetic Neurobiology Group, and Department of Biological Engineering, Massachusetts Institute of Technology, Cambridge, MA 02139.

[2]Department of Brain and Cognitive Sciences and MIT McGovern Institute for Brain Research, Massachusetts Institute of Technology, Cambridge, MA 02139.

Abstract

Optogenetics enables light to be used to control the activity of genetically targeted cells in the living brain. Optical fibers can be used to deliver light to deep targets, and LEDs can be spatially arranged to enable patterned light delivery. In combination, arrays of LED-coupled optical fibers can enable patterned light delivery to deep targets in the brain. Here we describe the process flow for making LED arrays and LED-coupled optical fiber arrays, explaining key optical, electrical, thermal, and mechanical design principles to enable the manufacturing, assembly, and testing of such multi-site targetable optical devices. We also explore accessory strategies such as surgical automation approaches as well as innovations to enable low-noise concurrent electrophysiology.

1. INTRODUCTION

Optogenetics has been widely applied to the control of single or small numbers of deep structures in the brain (e.g., using a fiber-coupled laser [1-4]), as well as to patterned control of superficial brain areas (e.g., using scanning lasers, LED arrays, and other 2-D patterning strategies (e.g., [5-7]). Recently we have engaged in developing devices that exhibit both the scalability to high target counts exhibited by 2-D arrays of light sources, and the deep structure targetability of optical fibers, by delivering the light from a 2-D array of custom-placed sub-millimeter-sized LEDs, into a set of custom-length optical fibers that are individually docked to LEDs [8, 9], even in wireless fashion [10]. A key advantage of this methodology is that these devices can be built and tested by individual groups using simple machining and assembly techniques. We here present the process for design and construction of LED arrays and LED-coupled optical fiber arrays, demonstrating the key engineering principles of design and fabrication

[+]Correspondence and requests for materials should be addressed to E.S.B. (esb@media.mit.edu)..

AUTHORS' CONTRIBUTIONS

J.G.B. designed and implemented the fiber-coupled LED array with assistance from A.G. B.D.A. assisted with surgery testing. E.S.B. contributed to technology designs and oversaw designs and experiments. J.G.B. and E.S.B. wrote the paper.

The authors declare no competing financial interests.

Such devices are compact and lightweight, and are easily carried by freely moving mice. Our design is centered around a procedure in which a 2-D LED array is assembled, and a set of custom-length fibers are docked to it, in a single step, thus enabling easy end-user customization and fabrication of a set of arrays in a matter of days, using inexpensive computer-based automated machining tools. We enable device operation for behaviorally relevant timescales, and can support electrophysiological recording concurrent with optical illumination. We describe new tools to systematize the surgery, facilitating good device insertion.

2. Materials and Methods

2.1 LED and Fiber-coupled LED Array Fabrication: Design and Preparation of Key Structural Components

Fiber arrays are made of an array of optical fibers (components **1** in **Figure 1A**), which are docked to a planar set of LEDs (components **2** in **Figure 1A**). The alignment of the fibers to LEDs is achieved via a stack of structural components (the fiber alignment plate, reflector plate, and LED base plate, components **5, 7,** and **11** in **Figure 1A**, respectively) that hold the optical elements (LEDs and optical fibers) in precise positions (within 10 microns) relative to guide holes on the structural components. The guide holes are aligned with device assembly guideposts (component **8** in **Figure 1A**) to hold the stack of structural components in the proper position. Detailed assembly instructions are given in the following sections, and the purpose of each component is explained in the Results, 3.1 Fiber array design, fabrication, and operation.

To facilitate the design and creation of fiber arrays, we developed a pipeline of computer aided design and fabrication tools. We use EAGLE, a free CAD program, to graphically lay out all of the components in the fiber array (see **Supp. Figure S1** for a schematic of the hippocampal CA1-targeted fiber array in EAGLE), and we use a tabletop, computer-controlled mill (MDX-15, from Roland DGA) to cut components **5, 7, 10,** and **11** (see **Figure 1A**) out of stock materials. MATLAB scripts act as a bridge between the design and fabrication processes, translating specifications for the arrays extracted from EAGLE into machine code readable by the mill. Crucially, EAGLE provides methods for automated data input, through script files, as well as automated data output, through its CAM processor. Thus, array specifications stored in a MATLAB script can be visualized and then adjusted in EAGLE, and changes made in EAGLE can be recorded in the MATLAB script. Details are provided in section **S3. Supplemental Methods: Fiber Array Design Guide**.

2.2 Fiber Array Fabrication: Preparation of Other Components

A number of other components must be prepared prior to assembly into a fiber array. Optical fibers (component **1** in **Figure 1A**) are prepared from 0.48 NA, 200 μm-diameter core optical fiber (Thorlabs) by sectioning into 1-inch-long segments with a razor blade and removing all jacketing with a wire stripper (Stripmaster). In order to facilitate reliable and repeated cleaving of fibers to desired length, a diamond fiber cleaver is used, in conjunction with fiber length trimming shims (milled according to the instructions in Supplemental Methods S3.4 Computer Aided Fabrication of Other Fiber Array Components), which are

small blocks that fit in a slot of the diamond cleaver and are milled to the length of each fiber. The fiber segment is inserted into a diamond fiber cleaver (Delaware Diamond Knives) against the back of the cleaver, and cleaved once. The fiber is then pushed forward within the cleaver the length of the shim of desired fiber length (i.e., by placing the shim between the fiber and the back of the cleaver), and cleaved again, producing an optical fiber the length of the shim with optically smooth cleaves on both ends. This process is repeated for each desired fiber.

Guide posts (component **8** in **Figure 1A**) are made of .020” stainless steel wire (Small Parts), cut into 1 cm lengths (e.g., using a Dremel abrasive wheel). Heat conduits (component **9** in **Figure 1A**) are made of 1/32” copper wire (McMaster-Carr), cut into 3 mm lengths.

2.3 Fiber Array Fabrication: Assembly

The first set of steps of device assembly is to put the LEDs and the circuit board (components **1** and **10** in **Figure 1A**) onto the LED base plate (component **11** in **Figure 1A**). The LED pedestals (component **3** in **Figure 1A**) are pre-tinned by depositing a thin layer of solder paste on top and then heating the LED base plates on a hot plate set to 235°C for 20 seconds. Then additional solder paste, as well as raw die LEDs (e.g., Cree EZBright Gen II EZ500, EZ600, EZ700, or EZ1000 chips), are put on the pedestals. At this time, we also place the circuit board (component **10** in **Figure 1A**) atop the LED base plate, with a thin sandwich of solder paste in between. The device assembly guideposts (component **8** in **Figure 1A**) are then inserted through the guidepost holes so as to align the circuit board to the LED base plate. Optionally, the fluidic cooling channel plate (component **13** in **Figure 4A**) and fluidic cooling channel backing plate (component **14** in **Figure 2A**) are attached to the LED base plate with solder paste. This assembly is heated on the hot plate for another 20 seconds, followed by guidepost removal after the solder has hardened. The electrical connector (component **12** in **Figure 1A)** (i.e. Samtec FTE10) is then soldered to the circuit board. A copper wire is inserted through the via (the top hole in the circuit board, **Figure 1B**) and soldered to both sides of the circuit board; this connects the positive voltage supply, coming from the electrical connector on the top side of the circuit board, to the plane of copper on the bottom side of the circuit board and the LED base plate, which provides the positive voltage source common to all the LEDs soldered onto the LED base plate. Finally, the assembled apparatus is cleaned of flux residue in a small plastic tube filled with isopropyl alcohol inside an ultrasonic bath.

The assembled apparatus is next hot glued to a glass slide with the coolant backing plate (for cooled arrays) or LED base plate (for uncooled arrays) flat against the slide. LED bond pads are wedge bonded to copper circuit board traces via 0.001” aluminum wire (using a wire bonder, West Bond 747677E-79C).

The remainder of the key structural parts, the alignment plate and the reflector plate (components **5** and **7** in **Figure 1A**), are linked by the four device assembly guideposts, and epoxied around the edges to insure a small (e.g., 1 mm) gap for thermal insulation. Reflector plate heat conduits are inserted into the reflector plate and attached with thermal epoxy.

Fiber fittings (component **6** in **Figure 1**, made from PEEK tubing 0.010” inner diameter, 0.018” outer diameter for the plates as designed above) are inserted through the alignment plate and reflector plate and cut flush with a razor blade on both sides, then set in place by filling the space between the alignment plate and reflector plate with epoxy. Then the optical fibers are loaded into the PEEK fiber fittings. This second assembly is then lowered onto the LED base plate so that the guideposts insert into the guidepost holes of the LED base plate, and the optical fibers are just above (~100 microns) the LEDs. Optics glue (Thorlabs) is then applied to the LED-fiber interface and cured with a UV lamp. The reflector plate heat conduits are bonded to the LED base plate with thermally conductive epoxy. The spaces in between the reflector plate, the circuit board, and the LED base plate are filled with 5-minute epoxy, and after curing, the guide posts are rotated about their own axes gently to loosen them from the epoxy, then pulled out of the device. To seal the outside of the device to insure biocompatibility, to prevent electrical shorts, and to block stray light from emitting, the exposed leads of the electrical connector are sealed with hot glue, and the surface of the device is coated with black epoxy. Finished arrays are released from the glass slides by placing the slides on a hot plate at 100°C until the hot glue attaching the array to the slide (described in the previous paragraph) becomes soft (this procedure does not affect the hot glue used to seal the exposed leads of the electrical connector). Finally, if cooling is used, barbed fluidic connectors (component **15** in **Figure 2A**, 3D-printed out of acrylic and threaded on the outside with a 0-80 die) are screwed into the holes in the coolant backing plate and sealed to the plate with epoxy.

For the bilateral CA1 14-fiber design (**Figure 1A-C**), we chose fiber termini (listed in the following list, in units of millimeters anterior, lateral, and ventral to bregma) of: (−1.70, ±0.60, 1.25), (−1.70, ±1.30, 1.00), (−2.40, ±1.50, 0.90), (−2.40, ±2.20, 1.10), (−3.10, ±4.10, 4.25), (−3.10, ±2.50, 1.20), (−3.80, ±3.85, 2.75), so that 14 LEDs were used with centered fibers; arrays were constructed both with and without cooling modules.

2.4 LED Driver Circuit Design and Operation

The LEDs can be controlled using a standard LED driver circuit with a transistor and current-limiting resistor connected to the cathode of each LED. Importantly, the anodes of the LEDs are all connected together on the LED base plate, and it is desirable to tie the LED base plate to earth ground. Therefore, the LED cathodes must be connected to a negative voltage supply. We built a custom circuit board to facilitate controlling the LEDs with ground-referenced digital logic signals (**Supplemental Figures S4 & S5)**.

2.5 Fiber Array Testing: Light Power

We measured light power output with n = 7 Cree EZ600 LEDs, each coupled to a 200 μm core-diameter, 0.48 NA optical fiber. Power measurements were performed with an integrating sphere photometer (Thorlabs). Arrays were fit in place over the integrating sphere (with original connector removed) with a lasercut adapter with a dock for the alignment plate, which blocked stray light from entering from the integrating sphere. Individual LEDs were run at 500 mA with water cooling (room temperature, 30 mL/min, with a peristaltic pump). Measured power was divided by optical fiber tip surface area to obtain irradiance.

2.6 Fiber Array Testing: Thermal Testing In Vivo

We measured temperature within the dental cement between a fiber array and the skull of a mouse (an acute experiment under isoflurane anesthesia, body temperature maintained with a heating pad). We tested two cooled hippocampal arrays (room temperature water coolant circulated through the cooling module with a peristaltic pump, 30 mL/min) and two uncooled arrays with two LEDs each, in each case with a disposable thermistor (Digikey part 495-2159-ND) embedded in the dental acrylic between the array and the skull. The thermistor was placed in a voltage divider circuit, and the thermistor voltage acquired by a NI-DAQ board, digitized at 10 Hz. We sampled the space of fiber array powers and fiber array durations of operation over a wide range of protocols of interest to neuroscientists. To facilitate further extrapolation to protocols not explicitly tested here, we additionally performed a curve fit for each of the two datasets (the cooled array dataset and the uncooled array set), modeling the system as undergoing two processes: fast-timescale dumping of heat into the system, and slower-timescale heat dissipation to the environment. A convenient approximation to these two guiding principles is simply to fit the empirical data with a two parameter equation that both captures the kinetics of heat generation and of heat dissipation; to first order, this can be written as

$$T = a^{*}P^{*}D / (1 + b^{*}D)$$

expressing temperature increase, T, as a function of the total fiber array power (as utilized in **Figure 3A**), P, the duration of fiber array operation, D, and two free parameters, a and b.

2.7 Fiber Array Fabrication: Optimization for Electrophysiology

Two sets of cables are needed for joint optical fiber array perturbation with concurrent recording: one to carry power to the LEDs and one to carry neural signals back (for this, a conventional cable is fine). For the power cables, we developed a novel style of coaxial cable (**Figure 3C**), which is designed to eliminate inductive and capacitive coupling to nearby surfaces and wires, Briefly, the outside comprises a tubular copper mesh (Daburn), held at ground (which eliminates capacitive coupling), that provides a current path from a power supply to the common anode of the LEDs; running inside the mesh is a bundle of twisted copper strands (33 gauge magnet wire, MWS Industries, twisted with a power drill) that serve as individual current return paths for each LED's cathode. For the internal copper wires, determining how the pins of the two male connectors correspond can be accomplished with a multimeter. Importantly, the helical copper strands and the tubular copper mesh are coaxial and carry equal and opposite currents, minimizing the inductive coupling between the cable and nearby recording devices.

2.8 Electrophysiological Recording and Data Analysis

We performed acute cortical recordings in an awake, headfixed mouse, using a LED-coupled fiber with a tetrode epoxied to the side of the fiber. To prevent photoelectrochemical artifacts [3, 11] from corrupting our measurement, during the construction of the device a thin opaque FR1 plate was placed between the LED and the end of the fiber. Neural signals were amplified 20× by a headstage amplifier and 50× by a

second stage amplifier (Plexon), digitized at 30 kHz with a Digidata (Molecular Devices), and analyzed with pClamp and MATLAB. After neural recordings were established, LEDs were then driven at 500mA for 10 ms pulse durations at 50 Hz for 300 ms train durations (i.e., 15 pulse repetitions), with a pulse train every five seconds, for 1 minute sessions. The same measurements were repeated with the tetrode and fiber tips in saline. For analysis of LED-electrode coupling, we analyzed the data obtained from 11 LED pulses that were delivered at 10 ms duration at maximum power, after at least 50 ms of darkness (3 electrodes, for a total of 33 total traces). We calculated average and standard deviation traces in MATLAB, aligning traces on the LED pulses. We computed the difference between the neural and saline artifact by subtracting the averaged saline artifact from each raw neural trace, and then averaging the resultant subtracted neural traces. To look for action potentials, traces were bandpass filtered between 270 and 8000 Hz.

2.9 Fiber Array Fabrication: Accessories for Surgery Practice and Surgery Facilitation

Molds for assembling practice arrays (see **Supp. Figure S2** for a picture of mold during assembly) are created from 1/16” FR1 epoxy laminate plates, each plate of which is milled separately (see S**upplementary Methods S3.4** for details on milling), and which are then stacked on top of each other, aligned with guideposts that go through holes milled in each of the four corners (and that stick out, for use in practice array assembly). Plates are secured to each other on the sides with hot glue. The key design feature of the practice array assembly mold, facilitated by the computer aided design and fabrication system, is that each component plate is milled to have holes that line up, in the final stacked assembly, to form columns through which fibers can be inserted, so that each fiber is immersed in the mold to a depth which equals its ultimate desired depth in the brain. To enable fibers to be inserted into these columns so that the centers of the fibers are precisely aligned, pieces of PEEK tubing (i.e., identical to the PEEK fiber fitting utilized above, component **6** in **Figure 1A**) are inserted into the plates as described in the above section; to facilitate replacement of PEEK tubing (e.g., if damaged) without having to remake the whole practice array mold, the PEEK tubing pieces can be mechanically constrained (e.g., by being inserted into a plate that is flanked above and below by plates with smaller holes than the outer diameter of the PEEK tubing).

Practice arrays (**Figure 4Bi**) are constructed by placing a practice array plate (essentially a fiber alignment plate, with holes drilled where the fibers pass through, with an extra tab sticking out, to facilitate later attachment of an electrical connector to enable mounting on the stereotaxic arm; see supplementary methods **S3.4** for details) over the practice array assembly mold, so that the guideposts pass through the guidepost holes in the practice array plate. Then, PEEK fiber fittings (component **6** in **Figure 1A**) are inserted into the holes in the practice array plate, and trimmed to the thickness of the plate. Optical fibers are stripped of their jacketing and inserted through the PEEK fiber fittings in the practice array plate, down into the practice array assembly mold until the fibers touch the bottoms of the columns that have been machined to insure that the appropriate lengths of fiber extends below the end of the practice array plate. Optical fibers are cut so that a few millimeters of fiber extend above the practice plate, and then hot glue is placed on top to hold the fibers and PEEK fittings to each other and to the plate. An electrical connector (identical to component **12** in

Figure 1A) is epoxied onto the top of the practice plate, to help with later holding by the stereotax during surgery. The practice array plate is encapsulated in biocompatible epoxy.

Parallelized craniotomy markers (**Figure 2Bii**), to aid in the stereotactic determination of coordinates for drilling craniotomies to insert fiber arrays into the brain, are constructed by supergluing PEEK fiber fittings into the holes of a practice array plate (see above and **Supplementary Table S1**). Hypodermic tubing (32 gauge, ~1 cm long) is cut and then inserted into the PEEK fiber fittings. An electrical connector (identical to component **12** in **Figure 1A**) is epoxied onto the top of the automated craniotomy marker, to help with later holding by the stereotax during surgery.

2.10 Fiber array implantation

All animal procedures were in accordance with the National Institutes of Health Guide for the care and use of Laboratory Animals and approved by the Massachusetts Institute of Technology Animal Care and Use Committee. Mice were anesthetized with isoflurane in oxygen, and then administered buprenorphine and Meloxicam for analgesia. After revealing the skull, and leveling bregma and lambda to the same vertical position, the sites for craniotomy opening were indicated by using a parallelized craniotomy marker (essentially an alignment plate with freely-moving hypodermic tubing inserted within, and dipped into sterile, biocompatible ink, see **2.9** for details) held by the stereotax and lowered, to mark the locations of all the drill sites in one step. Then three small screws (size 000, 3/32” long, J.I. Morriss) were implanted to make a broad-based tripod for attachment of the fiber array atop the skull [12]. Small craniotomies in the skull were made, over each ink-stained drill site, with a hand drill (e.g., Barrett pin vise, with HSD-75 drill bit); alternatively, a large craniotomy was made around the outline of the ink-stained drill sites with a dental drill. Then, the optical fiber array to be implanted was attached to a custom holder (essentially a Samtec connector on a post that plugged into the electrical connector of the fiber array, component **12** in **Figure 1A**), and then lowered using a stereotaxic apparatus (e.g., Kopf) so that the tips of the optical fibers were 250 microns above the target coordinates, as explained above. Then, the fiber array was secured to the three skull screws with dental acrylic; it is important to “loop” the wet acrylic over the array to mechanically secure everything together.

3. RESULTS

3.1 Fiber array design, fabrication, and operation

We have previously shown that arrays of LEDs, patterned on a substrate to match the shape of target brain regions and implanted above the surface of the cortex, can be used to control behavior with optogenetic stimulation[10]. These arrays, wirelessly controlled and powered, allow a freedom of movement impossible to achieve with optical stimulators tethered to distal lasers. Additionally, the method used to pattern the LEDs on the substrate achieves a packing density (<1 mm center-to-center) and precision (features to mount LEDs machined with 25 μm resolution) that would be extremely difficult to achieve with traditional stereotaxic methods of implanting individual optical fibers. Thus, we sought to develop a method for fabricating arrays of optical fibers to be coupled to our arrays of LEDs, in order

to target deep brain structures with the same precision we have employed to target surface structures.

One core innovation used here is an efficient, precise way of docking a large set of optical fibers, to a large set of LEDs arrayed on a planar surface, so that the resultant device can safely and effectively deliver light independently to a set of sites distributed in a three dimensional fashion in the mammalian brain (**Figure 1**). We chose our fiber-LED coupling strategy to maximize light throughput, choosing optical fibers to have maximum numerical aperture in order to couple in as much light as possible, and we chose LEDs to have maximum surface irradiance. The Lambertian emission pattern of LEDs implies that the ratio of LED area to fiber end surface area should be greater than one to maximize the amount of light carried by a fiber; thus, according to a theorem derived in ref. [13], LEDs and fibers should be in direct contact to maximize light coupling, without additional lenses. For example, placement of a 200 micron optical fiber (0.48 NA) onto a 600 micron × 600 micron LED (465 nm wavelength Cree EZBright600), with the small gap bridged by an index-matched adhesive (see **2.3 Fiber Array Fabrication: Assembly**), yielded a maximum irradiance at the free end of the fiber of 220 ± 10 mW/mm^2 (mean ± standard deviation; LED run at the less-than-maximal current of 500 mA; n = 7 LED-coupled fibers), matching fiber tip irradiances commonly used in vivo for safe illumination of opsin-bearing cells [1-3]. At this tip irradiance, a fiber can illuminate the edges of a >1 mm^3 volume to an irradiance of >1 mW/mm^2 (as reflected by computational models and experiments in refs. [1, 2, 14]), a light level at which many commonly used microbial opsins are significantly activated [14-17]. Thus, depending on the scientific goal at hand, LED-coupled fibers can be packed together to guarantee ‘tiling’ of brain structures (~750 microns apart, as in **Figure 1A-C**, a “dense” bilateral CA1 hippocampus targeting array), or spaced sparsely (~1.5 mm apart, as in **Figure 1D**, a “sparse” bilateral CA1 hippocampus targeting array). Detailed guidelines on how to lay out the geometry of such fiber arrays, optimizing LED and fiber placement are provided in Supplemental Methods S3.1 Choosing Coordinates for Fiber Arrays.

To fabricate a 3-D fiber array, we first fabricate a 2-D array of LEDs, using computer-aided circuit design and manufacturing tools, and then align and dock the set of optical fibers to the set of LEDs, in a single positioning step. This single positioning step tolerates alignment errors of several degrees thanks to the angle-independent irradiance of LEDs, in contrast to lasers which must be precisely aligned. We here describe the principles of the design; detailed step-by-step instructions for semi-automatically manufacturing the components and performing the assembly are given in **2.1-3 Fiber Array Fabrication** and Supplemental Methods S3.3 Computer Aided Fabrication of Key Structural Components. Notably, only two relatively inexpensive machines not commonly found in an ordinary neurophysiology lab are required, a tabletop mill and a wirebonder. Assembly proceeds in two phases: in the first phase of construction, raw die LEDs (component **2** in **Figure 1A**) self-assemble onto solder-coated planar pedestals (component **3**) to form a 2-D array of LEDs on a copper LED base plate (component **11**), and then LED terminals are wirebonded (component **4**) to an attached circuit board (component **10**); the circuit board bears copper traces for provision of power to individual LEDs, and a connector to connect the LED array to the outside world

(component **12**). In the second phase of construction, an alignment plate (component **5**) that firmly holds, via fitted pieces of tubing (component **6**), a set of optical fibers (component **1**) cleaved to lengths that correspond to the dorsoventral coordinates of brain targets, is then lowered onto the 2-D LED array along a set of assembly guideposts (component **8**); optical adhesive is used to couple fibers to their corresponding LEDs. Since LEDs will, even coupled, still emit light that escapes capture by the fiber, we laminate a highly reflective aluminum reflector plate (component **7**) onto the fiber alignment plate with thermally insulating epoxy. This reflector plate is then thermally connected to the LED base plate via copper heat conduits (component **9**), thus using the LED base plate as a high heat-capacity heat sink away from the mouse skull. Calculations indicate that this strategy reduces the heat delivered towards the skull by stray LED light by approximately two orders of magnitude, vs. a design without a reflector. Finally, exposed surfaces of the device are coated with biocompatible epoxy. For surgical practice, fiber arrays without LEDs can be very rapidly fabricated, as shown in **Figure 2Bi and Supp. Figure 2**, and described in 2.9 Fiber Array Fabrications: Accessories for Surgery Practice and Surgery Facilitation and S**upplemental Methods S3.4**.

Several key mechanical, optical, and electrical engineering innovations equip the device with the properties of easy end-user design and fabrication, good optical performance, compact size and small weight, low heat production, and low electrical noise production. For example, after brain targets are chosen by the user, the four key structural plates (components **5**, **7**, **10**, and **11** in **Figure 1A**) are all semi-automatically machined out of their respective materials by a tabletop mill, which is controlled by a PC that runs custom scripts (e.g,. in MATLAB) that convert LED coordinates into mill instructions (see Supplemental Methods S3.3 Computer Aided Fabrication of Key Structural Components for details). Precision machining of all core structural plates from a single set of parameters insures high precision of fiber location along medio-lateral and anterior-posterior axes (<10 micron variability). As another example, to place a large number of small raw LED dies onto the LED base plate to make up a 2-D array, we utilized a self-assembly strategy in which the surface tension of solder on the small LED pedestals (component **3** in **Figure 1A**) automatically orients all the LEDs into a flat and fully aligned state, enabling 2-D LED array fabrication in a single step. Once assembled, such a device occupies <0.5 cm^3 in volume, and weighs <1 g, and thus is easily carried by a freely moving mouse on its head.

To achieve the compactness of our device, we use the LED base plate (component **11** in **Figure 1A**) as not only the mechanical LED mount and heat sink, but also as the common anode for all the LEDs. To power LEDs wired in this way, we designed a custom LED driver circuit board to receive TTL pulses (from any commodity source, e.g., a NI-DAQ board) and then to trigger the board to transmit the appropriate power to control the LEDs (see **2.4 LED Driver Circuit Design and Operation** for a description of the circuit, **Supp. Figure S3 and S4** for a schematic and layout of the LED driver circuit). We designed a novel geometry for a multichannel coaxial cable (visible in **Figure 2C-D**, and schematized in **Figure 3B**) to provide power to the LEDs on the fiber array; this cable uniquely minimizes both capacitive and inductive coupling of electrical signals to nearby structures (e.g., recording electrodes, **Figure 3A**) while allowing for dozens of independent current-

carrying LED control lines in a flexible cable format; this cable is described in more detail in **2.4 LED Driver Circuit Design and Operation.** We use pulleys and a counterweight to offset the weight of the electrical cable (and, optionally, of the cooling tubing, described below), that enables practically free mouse movement (and could be used in conjunction with electrical and fluidic commutators, if necessary).

This compact, lightweight fiber array design can support the operation of one LED for ~7000 ms of continuous operation at 500 mA – or, operation of one LED for 7000 1 ms-duration pulses, 700 10 ms-duration pulses, etc. – before the material holding the array to the skull (e.g., dental acrylic) increases temperature from baseline temperature by 1°C (solid lines and filled circles in **Figure 4**). An equivalent amount of heat would be produced for any fiber array protocol of operation in which the total number of LEDs, multiplied by the average LED on time, equals 7000 LED-ms – thus 5 LEDs could each be run continuously for ~7000/5 = 1400 ms, or 10 LEDs could each undergo 700/10 = 70 10 ms-duration pulses. After the fiber array is run on a protocol of operation, the array rapidly cools to baseline temperature with a time constant of 3.8 ± 0.1 minutes (mean ± standard deviation; n = 2 arrays), meaning that the available 7000 LED-ms of device operation can be re-utilized every few minutes, appropriate for many behavioral paradigms. Note that if a fiber array protocol of operation involves slow heat generation compared to this time constant – that is, the LEDs are run at a low power level, or the LEDs are pulsed at a very low frequency, then such a protocol of operation can continue indefinitely (**Figure 4**, steep upper left part of each curve). To expand the range of fiber array protocols of operation possible, we devised a supplementary cooling module (shown in **Figure 2A**) that increases the maximum amount of energy that can be consumed on the device by an order of magnitude or more (dotted lines and filled diamonds in **Figure 4**). In this modified design, a microfluidic cooling channel plate (component **13**, with microfluidic cooling channel backing plate, component **14**, in **Figure 2Ai**) attaches to the back of the LED base plate to support water cooling of the device (via connectors, component **15** in **Figure 2Ai**, that connect to tubing that leads to a peristaltic pump). A modest cooling system (using 750 micron diameter channels, and room temperature water flowing at a constant rate of 0.5 mL/sec) enables a ~9× increase in the duration of the protocol of operation for one LED, or a ~5× increase in the duration of the protocol of operation for 10 LEDs; additionally, the time constant of array cooling speeds up to just 1.5 ± .5 minutes (measured for n = 2 arrays).

3.2 Implantation, utilization, and validation of fiber arrays in behaving mice

Surgical implantation of fiber arrays into the mouse brain takes place under anesthesia, after the insertion of three anchor screws into the skull [12]. We have begun the process of automating the surgery; for example, we mark all of the craniotomy sites needed for fiber array insertion in a single step by lowering onto the skull an array of free-sliding micro-pens so that each marks the location of a craniotomy with an ink dot (see **Figure 3Bii** and 2.9 Accessories for Surgery Practice and Surgery Facilitation)

3.3 Integration of electrophysiological recording and fiber array illumination

The fast pulses of current that power the LEDs of a fiber array can potentially result in artifacts on nearby conductors via capacitive and inductive coupling. To solve this problem,

we developed a lightweight multichannel coaxial cable to convey power to the LEDs (schematized in **Figure 4C**). The key design innovation is to have the internal wires of the cable spiral about the central axis of the cable, so that as seen from outside the cable, each individual internal wire spatially averages so as to simulate a true coaxial cable, in conjunction with an outer copper mesh. Currents (500 mA, 10 ms long) delivered to an LED on an array resulted in little noise on electrodes running along the corresponding fiber on the array. The small, low frequency artifacts that did couple in (average peak of 15 ± 4 μV, avg ± std. dev. across electrodes, n = 3 electrodes) were identical between recordings performed in saline and in vivo, enabling high-fidelity subtraction, leaving undetectable noise (**Figure 3B**).

4. DISCUSSION

We here present the design and fabrication methodology for a device that comprises an array of custom-length optical fibers docked to a 2-D array of LEDs[8-10], which enables independent light delivery to sites distributed in a three-dimensional pattern throughout the mammalian brain, important for targeting realistically-shaped brain circuits for neural perturbation. Our device possesses a form factor that is compact and lightweight enough (e.g., ~1 gram, ~0.5 cm^3) to be borne by freely moving mice. Each individual fiber can easily address a volume on the order of a cubic millimeter with irradiances on the order of 1 mW/mm^2; greater volumes are addressable at lower light powers. The device can be operated for periods of time appropriate for many behavioral experiments; when used in conjunction with a supplementary fluidic cooling apparatus, it can support experiments in which large numbers of LEDs are operated for long durations. For power delivery, our device utilizes a novel multichannel coaxial cable, which minimizes capacitive and inductive artifacts on adjacent neural recording electrodes. Finally, we devised new tools to systematize surgery, enabling large numbers of fibers to be inserted through targeted craniotomies.

To simultaneously achieve in a single device the many specifications required – three-dimensional targeting of light with good optical performance, easy end-user design and fabrication, compact size and small weight, low heating and electrical noise – required a large number of optical, mechanical, electrical, and thermal variables to be simultaneously optimized. For example, the coupling strategy between LEDs and fibers not only maximizes light throughput, but also enables single-step alignment of a large number of optical fibers to a 2-D LED array. The core structural plates of the device enable not only this single-step alignment process, but also provide for heat management, and support passive electrical noise cancellation. To create a batch of fiber arrays, from design to final assembly, takes a few days for an experienced practitioner, using just two inexpensive computer-controlled manufacturing devices in addition to what might be found in a modern neurophysiology laboratory.

Like other instruments that can be designed and assembled by end users (e.g., tetrode microdrives, etc.), virtually infinite possibilities abound for how these fiber arrays may be customized and augmented. Our device uses blue LEDs, appropriate for activation of not only opsins whose action spectra peak in the blue such as ChR2, Mac, and Chronos [18], but

also many other opsins such as Arch that have action spectra peaks in the green or yellow but are also well activated by blue light. In the case of Arch, for example, its sensitivity to light at 470 nm is approximately 50% of its peak sensitivity, still enabling very significant silencing in a region [14]. Other colors of LEDs may also be used, such as high-power 625 nm LEDs to drive the red-light sensitive silencer Jaws [19]. We expect that as consumer applications drive improvements in the components that make up the fiber array – e.g., LEDs become more efficient, digital fabrication becomes cheaper – the fiber array device itself will ride these technology development curves, becoming more powerful. Many other variants are conceivable: as one of many examples, the use of low-temperature fluids for array cooling, in conjunction with active thermistor feedback, could support the extending of the number of LEDs that can be operated on the array, and the durations of LED operation, to arbitrarily high levels. Commonly used neural recording devices can be integrated with our array: for example, tetrode bundles or silicon probes could be passed down through holes strategically placed in the array. In the years to come, we anticipate that new technologies, such as bundles of waveguides [20] coupled to miniaturized lasers, and novel surgical technologies such as machines that automatically drill craniotomies, will pave the way towards systematic deployment of such devices at even denser levels throughout distributed neural circuits. Such devices may also serve, in the future, as prototype optical neural control prosthetics, supporting the development of novel treatment strategies for intractable neurological and psychiatric disorders.

Supplementary Material

Refer to Web version on PubMed Central for supplementary material.

ACKNOWLEDGEMENTS

ESB acknowledges funding by the NIH Director's New Innovator Award (DP2OD002002) as well as NIH Grants 1RC1MH088182, 1RC2DE020919, 1R01NS067199 and 1R43NS070453, NSF (0835878 and 0848804), McGovern Institute Neurotechnology Award Program, Department of Defense CDMRP PTSD Program, Human Frontiers Science Program, NARSAD, Alfred P. Sloan Foundation, Jerry and Marge Burnett, SFN Research Award for Innovation in Neuroscience, MIT Media Lab, Benesse Foundation, and Wallace H. Coulter Foundation. JGB acknowledges the Hugh Hampton Young Fellowship. Thanks to Michael Hemann and Neil Gershenfeld and the Center for Bits and Atoms for use of their respective lab facilities.

REFERENCES

1. Aravanis AM, et al. An optical neural interface: in vivo control of rodent motor cortex with integrated fiberoptic and optogenetic technology. J Neural Eng. 2007; 4(3):S143–56. [PubMed: 17873414]
2. Bernstein JG, et al. Prosthetic systems for therapeutic optical activation and silencing of genetically-targeted neurons. Proc Soc Photo Opt Instrum Eng. 2008; 6854:68540H.
3. Han X, et al. Millisecond-timescale optical control of neural dynamics in the nonhuman primate brain. Neuron. 2009; 62(2):191–8. [PubMed: 19409264]
4. Adamantidis AR, et al. Neural substrates of awakening probed with optogenetic control of hypocretin neurons. Nature. 2007; 450(7168):420–4. [PubMed: 17943086]
5. Poher V, et al. Micro-LED arrays: a tool for two-dimensional neuron stimulation. J. Phys. D: Appl. Phys. 2008; 41:094014.
6. Xu H, et al. Integration of a matrix addressable blue/green LED array with multicore imaging fiber for spatiotemporal excitation in endoscopic biomedical applications. physica status solidi (c). 2008; 5(6):2299–2302.

7. Ayling OG, et al. Automated light-based mapping of motor cortex by photoactivation of channelrhodopsin-2 transgenic mice. Nat Methods. 2009; 6(3):219–24. [PubMed: 19219033]
8. Bernstein JG, Boyden ES. Optogenetic tools for analyzing the neural circuits of behavior. Trends Cogn Sci. 2011; 15(12):592–600. [PubMed: 22055387]
9. Bernstein JG, Garrity PA, Boyden ES. Optogenetics and thermogenetics: technologies for controlling the activity of targeted cells within intact neural circuits. Curr Opin Neurobiol. 2011
10. Wentz CT, et al. A Wirelessly Powered and Controlled Device for Optical Neural Control of Freely-Behaving Animals. Journal of Neural Engineering. 2011; 8(4):046021. [PubMed: 21701058]
11. Ayling OG, et al. Automated light-based mapping of motor cortex by photoactivation of channelrhodopsin-2 transgenic mice. Nat Methods. 2009
12. Boyden ES, Raymond JL. Active reversal of motor memories reveals rules governing memory encoding. Neuron. 2003; 39(6):1031–42. [PubMed: 12971901]
13. Hudson MC. Calculation of the Maximum Optical Coupling Efficiency into Multimode Optical Waveguides. Applied Optics. 1974; 13(5):1029–1033. [PubMed: 20126127]
14. Chow BY, et al. High-performance genetically targetable optical neural silencing by light-driven proton pumps. Nature. 2010; 463(7277):98–102. [PubMed: 20054397]
15. Han X, Boyden ES. Multiple-color optical activation, silencing, and desynchronization of neural activity, with single-spike temporal resolution. PLoS ONE. 2007; 2(3):e299. [PubMed: 17375185]
16. Wang H, et al. High-speed mapping of synaptic connectivity using photostimulation in Channelrhodopsin-2 transgenic mice. Proc Natl Acad Sci U S A. 2007; 104(19):8143–8. [PubMed: 17483470]
17. Boyden ES, et al. Millisecond-timescale, genetically targeted optical control of neural activity. Nat Neurosci. 2005; 8(9):1263–8. [PubMed: 16116447]
18. Klapoetke NC, et al. Independent optical excitation of distinct neural populations. Nat Methods. 2014; 11(3):338–46. [PubMed: 24509633]
19. Chuong AS, et al. Noninvasive optical inhibition with a red-shifted microbial rhodopsin. Nat Neurosci. 2014; 17(8):1123–9. [PubMed: 24997763]
20. Zorzos AN, et al. Three-dimensional multiwaveguide probe array for light delivery to distributed brain circuits. Opt Lett. 2012; 37(23):4841–3. [PubMed: 23202064]

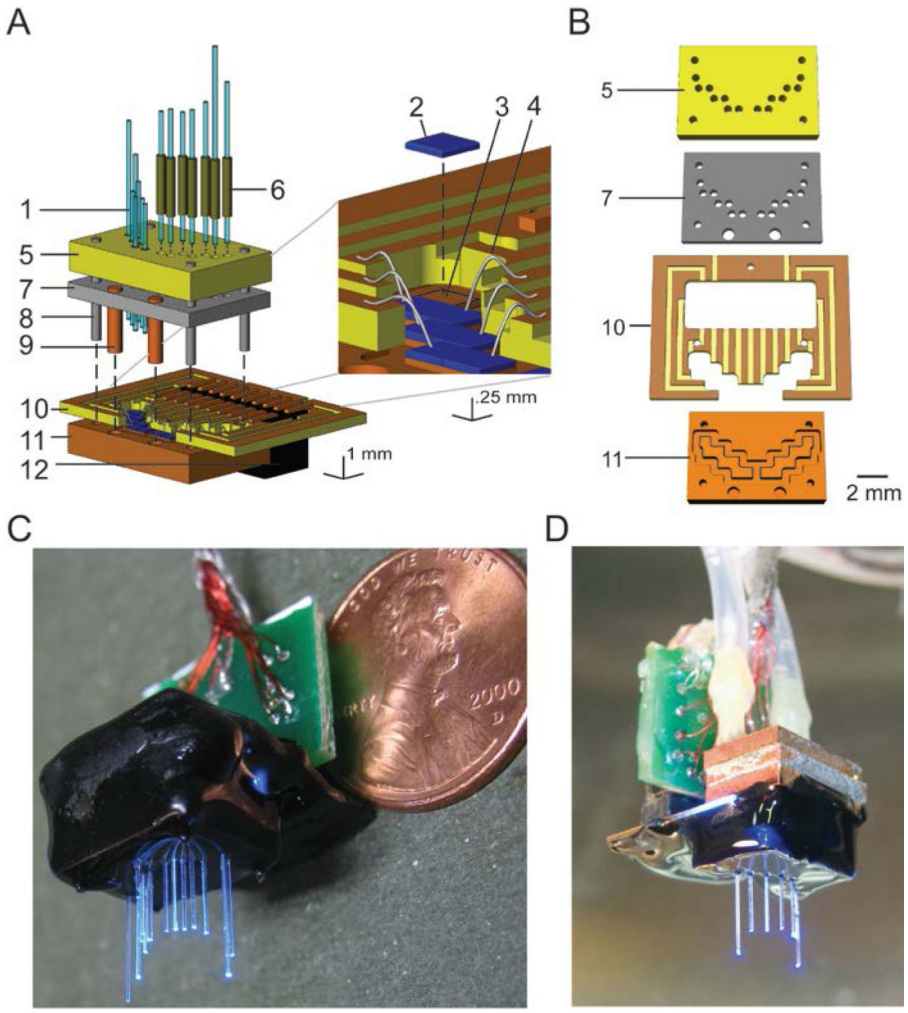

Figure 1. Design and fabrication of optical fiber arrays

A, Schematic, in exploded view, of a fiber array with fibers pointing upwards, with *inset* zoomed in on LEDs and their connections, adapted from refs. [8-10]. Vertical dashed lines denote points at which components dock together when the device is assembled. Numbers refer to key components: 1, optical fiber; 2, LED; 3, LED pedestal (carved out of LED base plate, 11); 4, wire bond; 5, fiber alignment plate; 6, fiber fitting; 7, reflector plate; 8, device assembly guidepost (to be removed after final assembly, but before implantation); 9, reflector plate heat conduit; 10, circuit board; 11, LED base plate; 12, circuit board connector. **B,** Key structural components, numbered the same as in **A**. **C,** Photograph of a relatively dense hippocampal CA1-targeted fiber array device (schematized in **A**), appropriate for silencing the entire hippocampus for example, with fibers pointing downwards, with a penny for scale. **D**, An 8-fiber hippocampal array, appropriate for stimulating multiple points in the hippocampus, shown with optional cooling module before encapsulation with biocompatible epoxy.

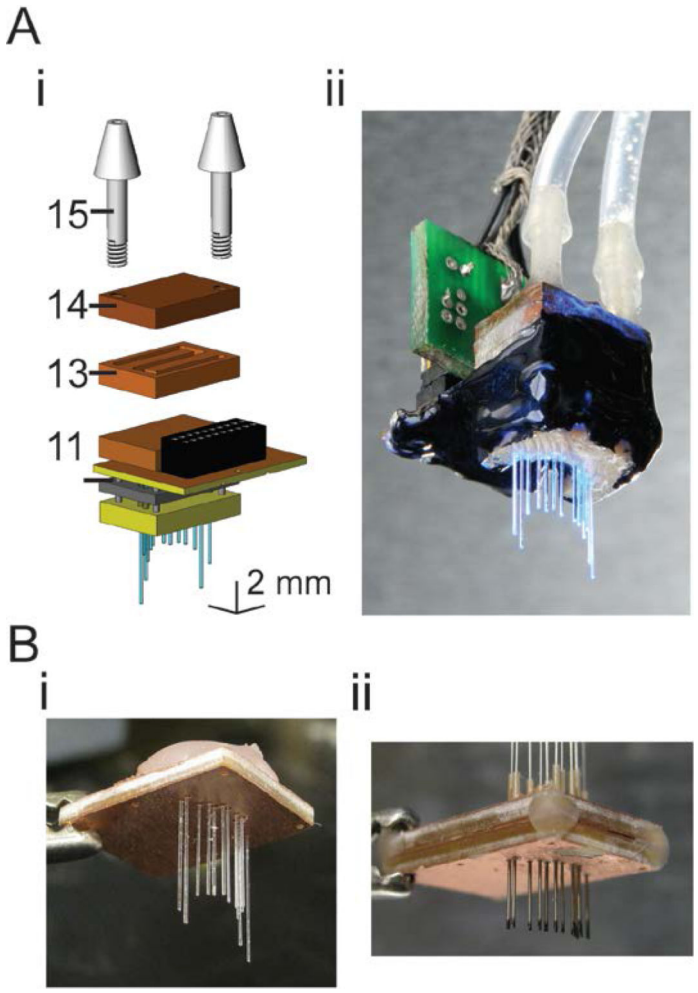

Figure 2. Accessory devices, and modifications, for implantation and utilization of fiber arrays

A, Fluidic cooling system, added to the back of the fiber array, appropriate for increasing the amount of time the array can be run continunously. **i,** Schematic, in exploded view, of the cooling system, added to the back of the fiber array. Numbers refer to key components: 11, LED base plate; 13, fluidic cooling channel plate; 14, fluidic cooling channel backing plate; 15, barbed fluidic connector. **ii**, Photograph of a cooled hippocampal CA1-targeted fiber array (based on the design in **Figure 3Ai**). **B,** Accessory devices to aid fiber array implantation. **i,** Practice array, with the same targets as the array schematized in **Figure 2A,** shown during fabrication before encapsulation with biocompatible epoxy. **ii,** Parallelized craniotomy marker, consisting of freely-moving hypodermic steel tubing with inked tips, appropriate for conforming to the contours of the skull and marking sites of craniotomies for fibers.

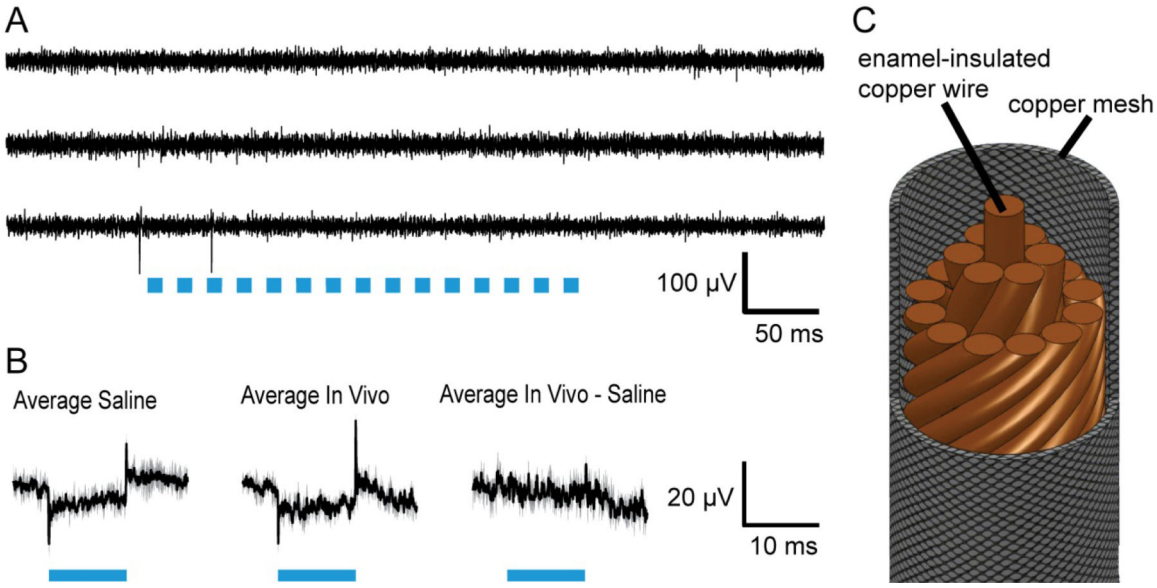

Figure 3. A custom coaxial cable design enables decoupled LED activation and recording

A, Raw traces of three electrode recordings on a tetrode (the fourth electrode here acts as amplifier reference), of neurons in the cortex of an awake headfixed mouse (non ChR2-expressing) during 50 Hz LED operation (each pulse was for 10ms at 500mA, indicated by blue bars). **B**, Average, across trials and electrodes, of 33 traces obtained in each of the saline (*left*) and in vivo (*middle*) conditions, displayed as mean (solid lines) ± standard deviation between electrodes (shaded area). *Right*, average of the 33 traces obtained in vivo, after each trace was preprocessed by subtracting off the saline-characterized artifact recorded on the same electrode (and averaged across all trials for that electrode, e.g. 11 trials). **C**, Schematic of the "spatially averaged" multichannel coaxial cable utilized to deliver power to LEDs while minimizing capacitive and inductive coupling to recording electrodes.

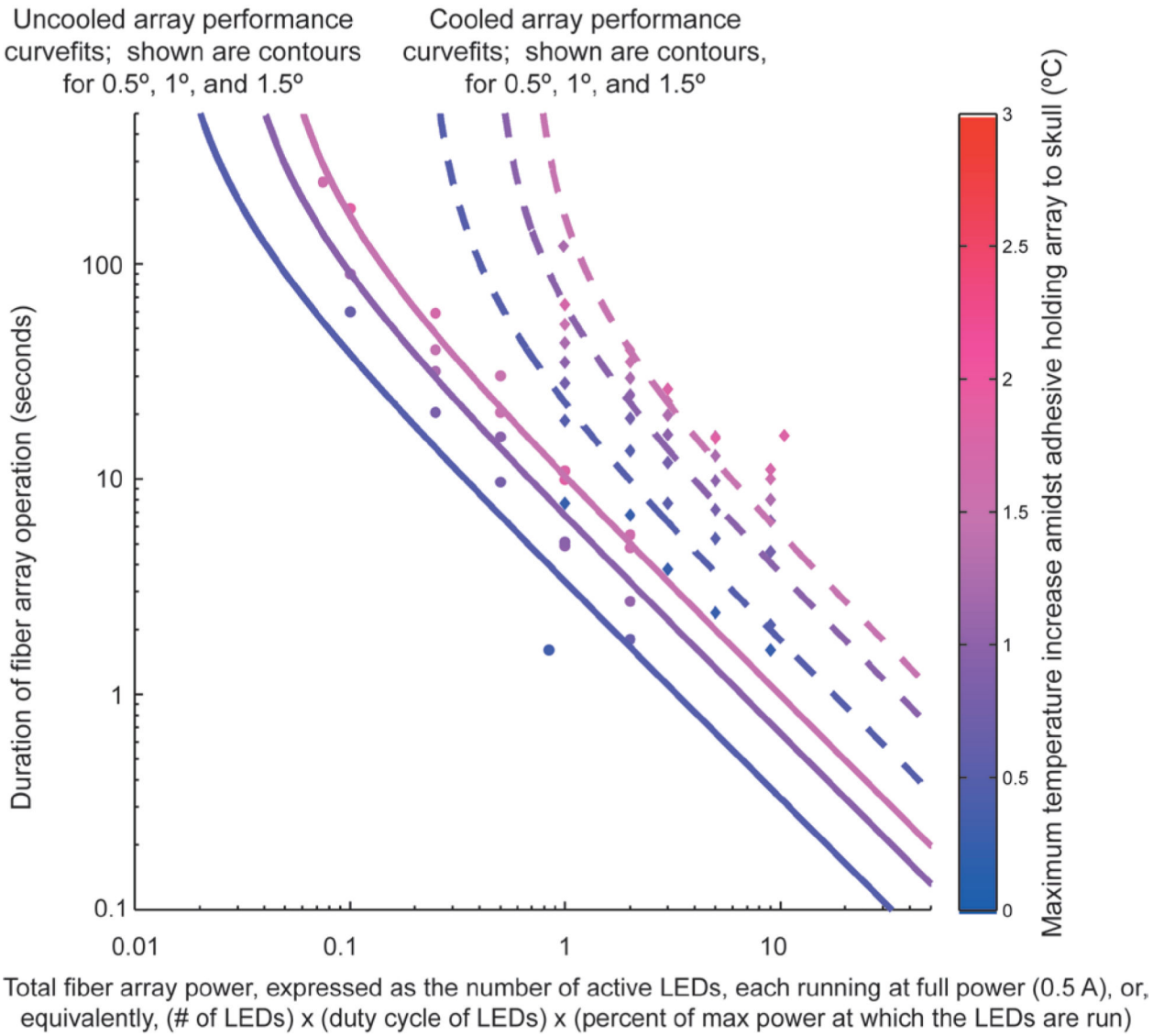

Figure 4. Thermal characteristics of fiber array use

Maximum temperature increase at a point in the material (dental acrylic) holding an array to the skull of an anesthetized mouse, for uncooled (solid lines, circles, n = 2 arrays) or cooled (dotted lines, diamonds, n = 2 arrays) fiber arrays, plotted as a function of the total fiber array power (x-axis, expressed in units of the number of active LEDs running at 500 mA) and the duration of fiber array operation at that given total fiber array power (y-axis). Shown for clarity is the behaviorally relevant portion of the temperature increase dataset acquired (circles, diamonds), as well as mathematically fit isothermal contours of temperature increase by 0.5, 1.0, and 1.5 °C.